Electronic Supplementary Material (ESI) for Soft Matter.


# Electronic Supplementary Information:

# Sequential deposition of microdroplets on patterned surfaces

Pallav Kant, Andrew Hazel, and Alice Thompson
*School of Mathematics, University of Manchester,*
*Oxford Road, Manchester M13 9PL, United Kingdom*

Mark Dowling
*Cambridge Display Technology Limited, Unit 12, Cardinal Business Park, Godmanchester,*
*Cambridgeshire PE29 2XG, United Kingdom (Company Number 02672530)*

Anne Juel*
*School of Physics and Astronomy, University of Manchester,*
*Oxford Road, Manchester M13 9PL, United Kingdom*
(Dated: August 27, 2018)

* anne.juel@manchester.ac.uk

# I. PREPARATION AND CHARACTERISATION OF SUBSTRATES

## A. Type-I substrates : Surfaces with topographical features and uniform wettability

The photo-lithographic process employed to fabricate type-I substrates is shown in Fig. S1. (i) Glass substrates were cleaned using a mixture of high-pressure deionized water and an ammonia-based solution to remove particles, followed by treatment with UV light and ozone for several minutes to remove organic contaminants. (ii) The cleaned substrates were subsequently coated with an approximately 1.3 $\mu$m thick layer of optically transparent proprietary negative-type photo-resist. (iii) This coated layer was then given a flood UV exposure (without the presence of a photo-lithography mask), followed by a brief post-exposure bake to 110°C and a 10 minutes curing bake at 205°C, both on hotplates. This treatment induced strong cross-linking of the photo-resist and provided a base to the pixel wells. (iv) The banks surrounding a pixel were created from a second approximately 1.3 $\mu$m thick layer of the same photo-resist used for the base layer, thus minimising any contact angle differences between the two. (v) This layer underwent exposure to UV, this time through a glass mask coated with a patterned Cr (chromium) layer which defined the stadium-shaped patterns, thus allowing the transfer of geometrical features onto the exposed area of the photo-resist. (vi) Following a brief post exposure bake to 110°C on a hotplate, the unexposed areas of the photo-resist were removed using a commercial developer solution, and the resulting patterned region hardened through a curing bake at 205°C for 10 minutes on a hotplate.

The height profile of the pixel side-wall was imaged using Scanning Electron Microscopy (SEM); see Fig. **??**. The angle between the flat bottom surface of the pixel and its side-wall was measured to be $\psi = 155° \pm 1°$. The same value was independently measured by contact stylus profilometry (Dektak 150), within an accuracy of 1°. In addition, we used contact stylus profilometry to probe the surface roughness of the fabricated surfaces, which were found to exhibit an average roughness of less than 5 nm.

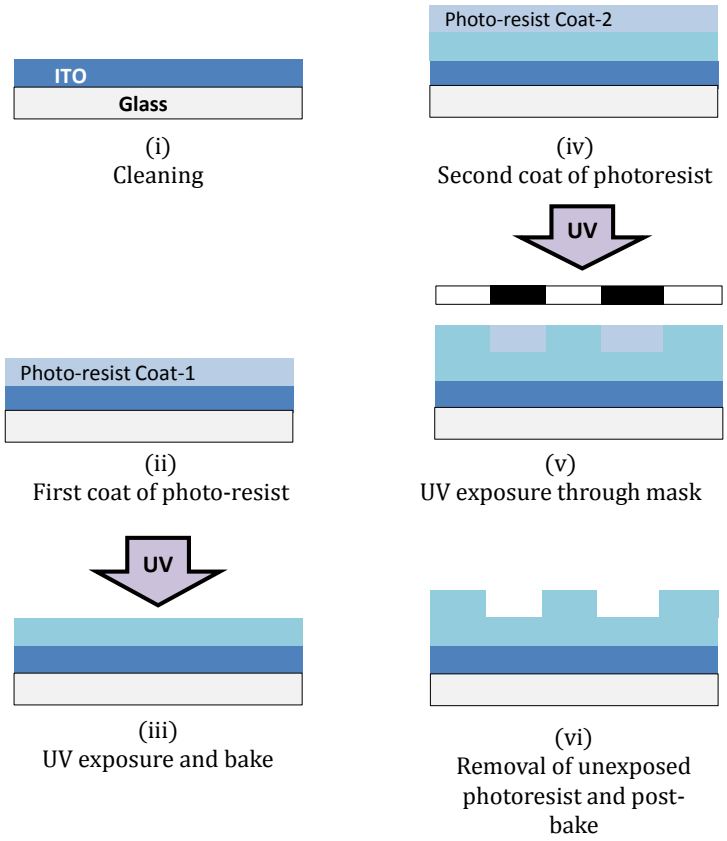


FIG. S1. Description of the photo-lithographic process used to make type-I substrates.

### B. Type-II substrates : Surfaces with both topographical and wettability patterning

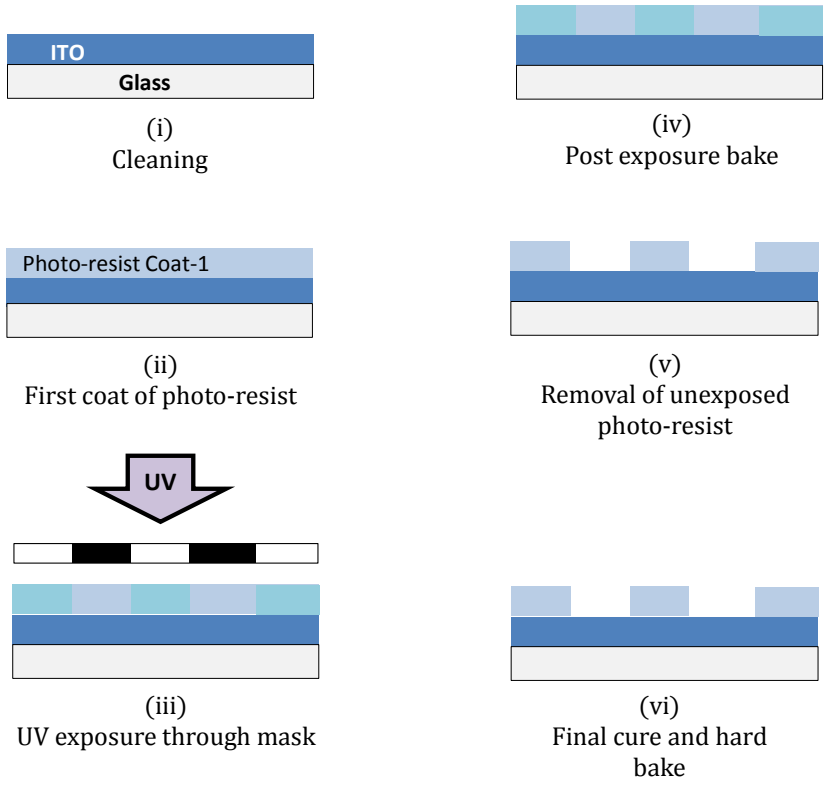


FIG. S2. Description of the photo-lithographic process used to make type-II substrates.

The photo-lithographic process employed to fabricate type-II substrates is shown in Fig. S2. (i) The glass substrates coated with a thin layer (50 nm) of ITO (Indium-Tin Oxide) were cleaned with high-pressure deionized water and an ammonia-based solution to remove particles, before exposing them to UV light to remove organic contaminants. (ii) The cleaned substrates were coated with an approximately 1.2 $\mu$m thick layer of optically transparent proprietary negative-type photo-resist. This photo-resist formulation contained a small amount (less than 1%) of fluorinated polymer, which made the surface less wetting to the liquid used in the experiments. (iii) The coated layer of photo-resist was baked on a hotplate at 110°C for a few minutes, before exposing it to UV for a few seconds through a carefully aligned glass mask with a patterned Cr (chromium) layer which defined the stadium-shaped patterns. This exposure of the photo-resist to UV through the patterned glass mask allowed the transfer of the geometrical features onto the exposed area and induced strong cross-linking of the photo-resist. (iv) To enhance and stabilise the chemical change in the exposed regions of the photo-resist layer, it was baked on a hotplate at 110°C for 10 minutes. (v) The unexposed parts of the photo-resist were removed by spraying of a proprietary developer solution, followed by the rinsing of the substrate in deionized water. These regions formed the inner surface (ITO coated glass) of the pixel. (vi) Finally, the photo-resist was baked for 10 minutes at 200°C, in order to harden the topographic profile of the side-walls and bring the small amount of fluorinated polymer from the bulk of the layer to its surface, thus increasing the advancing and receiding contact angles of the banks surrounding the pixel.

## II. FLUID REDISTRIBUTION AFTER THE DEPOSITION OF A DROPLET

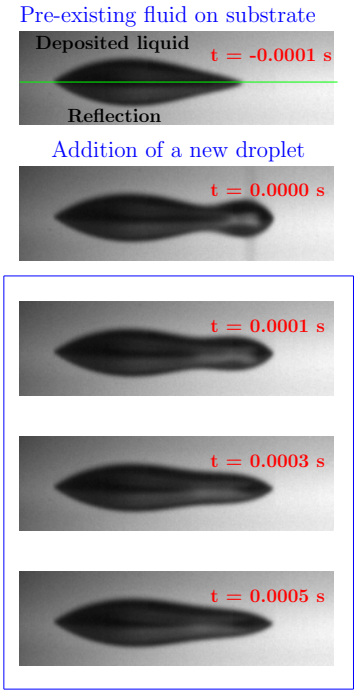


FIG. S3. Sequence of images illustrating the redistribution of added fluid immediately after the deposition of a drop. Images were recorded in side view at 10,000 fps, during the deposition of droplets on a flat substrate with $\theta_A(\theta_R) = 50^\circ(0^\circ)$ ($f = 500$ Hz; $v = 10$ mm s$^{-1}$; $\Delta x = 20$ $\mu$m).

## III. SMOOTHING OF THE CONTACT LINE FOLLOWING DROPLET DEPOSITION

In the numerical model, the addition of a circular footprint that partially overlaps the printed line results in a cusp at the point where the contact lines of both fluid regions intersect. However, in the experiment, the newly coalesced droplet was always smoothly connected to the footprint of the pre-existing printed line, see Figure 3(b). This suggests that the cusp in the contact line is smoothed out on time-scales shorter than our observation time due to early-time impact-driven spreading of the interface. We mimic this smoothing by replacing the contact line in the vicinity of the cusp by a third order polynomial that connects the footprint of the pre-existing fluid and newly deposited droplet, while retaining a constant total volume in the liquid layer.

We tested different lengthscales ($l$) of smoothing on the receding motion of a droplet newly deposited partially ouside the pixel boundary. In Fig. S4(a), smoothing is applied in the close vicinity of the cusp ($l \sim 0.2R_p$), resulting in a smooth neck connecting the newly deposited droplet ot the exisiting morphology. In Fig. S4(b), smoothing is applied to a larger section of the contact line ($l \sim R_p$) near the cusped region, resulting only in a slight indentation of the contact line. In (a), the evolution of the smoothed initial state results in a cusped contact line that comes to rest on the bank, while in (b) the contact line remains smooth and rounded, and closely matches the footprint observed in the experiments shown in Fig. S4(c). Hence, the smoothing shown in (b) was systematically applied in all the computations.

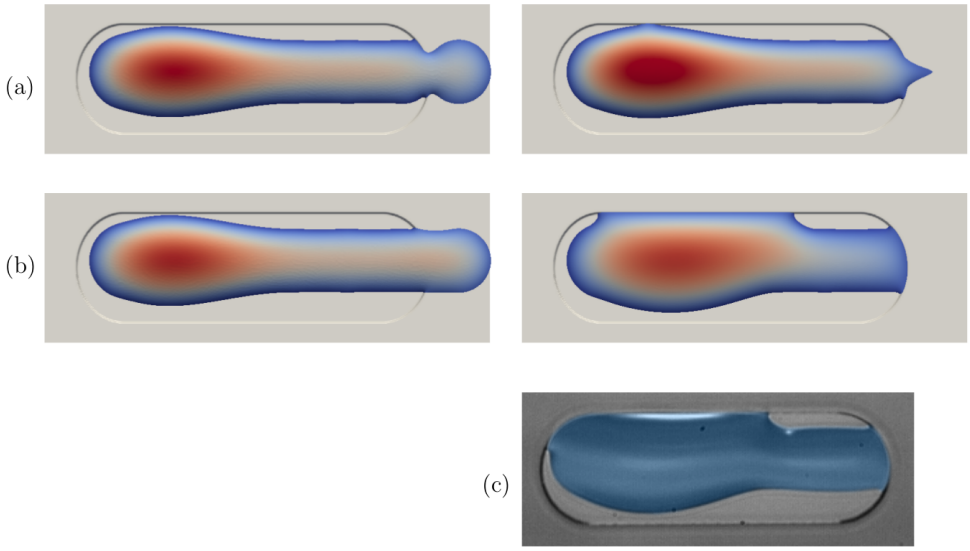


FIG. S4. Evolution of the liquid morphology for two different initial conditions after addition of a new drop partially outside the pixel boundary. (a) Smoothing is applied to the contact line within the lengthscale $l \sim 0.2R_p$ of the location of the cusp. The resulting footprint boundary exhibits a smooth fluid neck instead of a cusp. The evolution of the footprint results in a cusped interface that comes to rest on the bank. (b) Smoothing is applied to a larger section of the contact line ($l \sim R_p$) near the cusp, resulting in a footprint boundary without only minor indentation. The evolution of the footprint closely matches the experimental observation shown in (c). The colour scheme in the numerical results indicates the height of the fluid interface relative to the substrate, which is maximum in the centre of the footprint (red shade) and minimum at the contact line (blue shade).